PHYSICAL REVIEW E **77**, 010501(R) (2008)

Impeded structural relaxation of a hard-sphere colloidal suspension under confinement

Prasad S. Sarangapani and Yingxi Zhu*

Department of Chemical and Biomolecular Engineering, University of Notre Dame, Notre Dame, Indiana 46556, USA

(Received 12 April 2007; revised manuscript received 31 May 2007; published 17 January 2008)

The phenomenon of glass transition, such as the anomalous divergence in viscosity without apparent structural change, remains inadequately understood. We employ spatial confinement to probe length scale dependence on structural relaxation and concomitant glassy dynamics of a hard-sphere poly-(methyl methacrylate) colloidal suspension via confocal microscopy. Remarkable film thickness dependent scaling behavior is observed, where the mobility and relaxation processes of a "fluid" suspension are found to be significantly impeded as film thickness is reduced below 15–20 particle layers.

DOI: 10.1103/PhysRevE.77.010501 PACS number(s): 82.70.Dd, 64.70.P−, 68.15.+e

Glassy materials are an intriguing class of amorphous solids which are typically formed by quenching liquids well below their freezing temperatures to rigidity, yet bypassing crystallization. Numerous experimental and theoretical investigations have sought to understand the complex phenomenon of the glass transition, such as the divergence of viscosity and relaxation times in the "supercooled" regime, yet the physics of this phase transition remains widely debated [1,2]. Understanding the properties of the glass transition will lead to insight into disordered systems in general with their broad applications ranging from photonic materials synthesis to protein folding [1–4].

Theoretical work on glass-forming liquids by Adam and Gibbs [5] attributes the viscosity growth to the existence of "cooperatively rearranging regions" (CRRs) whose characteristic length scale grows upon rapid cooling. As free volume restrictions become significant due to the increase in the sizes of CRRs, particles cannot relax independently and move as cooperative groups to achieve structural relaxation. Consequently, structural relaxation is impeded. The validity of the Adam-Gibbs theory has been examined mainly with glass-forming molecular fluids [6] and recently with model colloidal suspensions [7,8]. However, defining such characteristic length scales as hallmarks of the glass transition remains a subject of great contention [9–12].

We employ confinement as an experimental approach to explore length-scale dependence on glassy behavior of a colloidal suspension, by which a dimensional reduction impedes structural relaxation while temperature and volume fraction are kept constant. This approach allows us to probe how the structure and dynamics of a bulk fluid colloidal suspension are modified as film thickness approaches a dimension comparable to the particle size. Of particular interest, the origins of cooperatively rearranging regions can be explored, as constrained motion of confined colloidal particles may result in a phase shift from a fluid to an apparent ''supercooled'' regime; particles thus follow one another in a cooperative fashion to achieve structural relaxation until the glass transition is approached where motion is "frozen in." We thereby probe a critical length scale upon a transition from an ergodic fluid to a nonergodic glass state by spatial confinement, where film thickness provides an additional length scale to understand the divergence in viscosity near the glass transition. We also examine the film thickness dependence of several time scales, such as cage rearrangement time as well as the α- and β-relaxation times, for structural relaxation.

The effect of confinement on the glass transition of polymeric thin films has been studied extensively, where the measured T_g and relaxation times under confinement increase or decrease from the bulk values depending on the cooling rate [13–16]. Experiments by the modified surface forces apparatus with a nanorheometer [17,18] reveal a glasslike transition for confined molecular fluids, where the longest relaxation time diverges as film thickness reduces. However, these measurements are ensemble averaged over film thickness and only provide indirect information regarding the packing configuration and dynamics of polymeric thin films.

In this Rapid Communication, we focus on the confinement induced glass transition of a model hard-sphere colloidal suspension where the packing configuration and dynamics are directly visualized by confocal microscopy at a single particle resolution. We report strong film thickness dependent glassy behavior of confined colloidal suspensions, in which colloidal particles in an initially fluid state show a significant reduction in their mobility and undergo a glasslike transition as film thickness becomes comparable to the particle diameter. In the range of volume fractions we explore, scaling behavior is evident: the onset of slow, glasslike dynamics occurs when film thickness, H, normalized by particle diameter, d, is reduced to $H/d=15-20$. Furthermore, a glass transition is induced at $H/d \leqslant 10$, where the measured α-relaxation time diverges. These results suggest a remarkable free-volume effect on structural relaxation.

A hard-sphere colloid, synthetic poly-(methyl methacrylate) (PMMA) ($d=1.2$ μm, polydispersity $<5\%$), sterically stabilized and fluorescently labeled with Rhodamine 6G ($\lambda_{ex}=488$ nm), suspended in a mixture of decalin and cyclohexyl bromide, are prepared through a procedure described elsewhere [19]. The suspensions are nearly index of refraction ($n=1.5$) and density ($\rho=1.225$ mg/ml) matched, thus minimizing particle sedimentation and light scattering. The volume fractions, ϕ of confined suspensions are determined by counting the number, n, of fluorescent particles present in the viewing volume, V, of confocal micrographs via centroid finding algorithms [20] and calculated as: $\phi=n\pi d^3/6V$. Bulk

*yzhu3@nd.edu

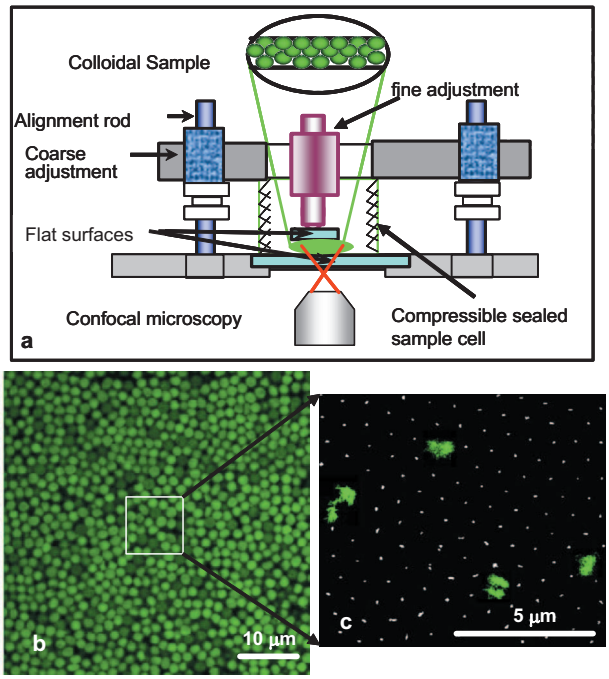

FIG. 1. (Color) (a) Schematic diagram of the compression sample cell that is mounted on the stage of an inverted confocal microscope. (b) Fluorescent micrograph of PMMA suspension of $\phi=0.57$ confined at normalized film thickness, $H/d=4$ and (c) corresponding trajectories of confined particles obtained from particle tracking where one-quarter of the entire scanning area is represented. Single-particle trajectories (green) are magnified.

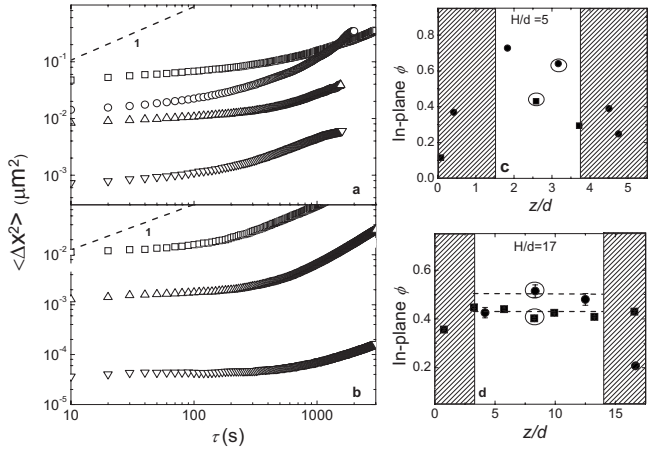

FIG. 2. Mean-square displacements (MSD) of confined PMMA suspensions for (a) $\phi=0.43$, highly fluidized suspension, for the bulk ($H/d\approx100$) (squares), and film thickness $H/d=25$ (circles), 17 (upper triangles), and 4 (down triangles), and (b) $\phi=0.57$, a "supercooled" suspension according to the hard-sphere phase diagram [11], for the bulk ($H/d\approx100$) (squares), and $H/d=17$ (upper triangles) and 5 (down triangles). In-plane volume fraction of confined colloidal thin films is examined against positions in the z direction away from the bottom surface for PMMA suspensions of $\phi=0.43$ (squares) and 0.57 (circles) at $H/d=5$ and 17, as shown in Figs. 2(c) and 2(d), respectively. Shaded areas in Figs. 2(c) and 2(d) indicate the depletion layers, which are excluded from our data analysis, and the circled datum points indicate the midplanes chosen for 2D dynamic characterization.

volume fractions, $\phi=0.40-0.61$ of PMMA suspensions, which range from a fluid regime up to a glass regime according to the hard-sphere phase diagram [10], are studied in this work.

We use a custom-built compression apparatus mounted on the sample stage of an inverted confocal laser scanning microscope (Zeiss LSM 5 Pascal, objective lens 63x, NA=1.4) to directly observe the structure and dynamics of confined colloidal thin films, as shown in Fig. 1(a). To reduce the depletion of PMMA from smooth glass surfaces, a thin layer of undyed PMMA is sintered at $\sim80\,^{\circ}$C (cf. $T_{m,\mathrm{PMMA}}=130\,^{\circ}$C) on a glass coverslip for three hours to roughen the confining surfaces and enhance particle-surface interaction. Suspensions are injected into a compressible sample cell by a pipette and sealed with UV-curing glue. The sample cell is then mounted on the confinement apparatus and left undisturbed for ~30 minutes before measurements. We systematically decrease film thickness stepwise. Film thickness is determined by both the readings of micrometers and confocal z-stack profile with an accuracy of ±0.1 μm [21]. Images of the confined suspension are recorded in time series at an interval of 1–5 s over a scanning area of 47×47 μm^2, where a representative image from our experiments is shown in Fig. 1(b) [21]. Wall effects are mitigated by acquiring images at the midplanes of the colloidal thin films. Typical particle trajectories for a strongly confined thin film are illustrated in Fig. 1(c).

To provide direct evidence of how confinement alters the mobility of colloidal suspensions, we start with a PMMA suspension of $\phi=0.43$, which is in the fluid phase with highly mobile particles in the bulk. The particle mobility is quantified in terms of the mean-square displacement (MSD) as

$$\langle\Delta x^2\rangle=\frac{1}{N}\sum_{j=1}^{N}\langle((x(t)-x(\tau))^2\rangle, \tag{1}$$

which is averaged over all particles and initial times, t, along the x coordinate [22,23], where N is the number of particles in the scanning area and τ is the lag time. Figs. 2(a) and 2(b) show the computed $\langle\Delta x^2\rangle$ against τ at varied film thickness for $\phi=0.43$ and 0.57, respectively. As film thickness decreases to $H/d\approx17$ for the sample of $\phi=0.43$, a marked reduction in the particle mobility is observed. Particles are trapped in cages formed by their neighbors for long times; subsequently, long-time diffusive behavior is observed for $\tau>100$ s when particles escape their cages [23].

To verify the generality of this confinement-induced phase shift, we also examine a dense suspension, $\phi=0.57$, which is in the "supercooled" regime and close to the colloidal glass transition. As shown in Fig. 2(b), a similar confinement effect on PMMA mobility is observed. Indeed, the mobility is consistently reduced with decreasing film thickness and the onset of the confinement effect shifts to greater film thickness at higher volume fractions. Additionally, it is intriguing to observe that the plateau in MSD is lower in magnitude and extends over longer lag times at a reduced film thickness, suggesting severely constrained particle motion with little

change in cage topology. The film thickness dependence of the onset of slow dynamics might be coupled with the "Lindemann length" associated with cage rattling near the glass transition [8], which typically decreases as volume fraction increases, or in our case, as film thickness is reduced. The Lindemann rule is a reliable criterion to infer cage topology from the vibration amplitude of a particle, which can be obtained from its mean-square displacement [8]. In our study, we expect that a reduction in free volume at a lesser film thickness could considerably affect relaxation dynamics where colloidal particles cannot relax independently and instead facilitate motion in a cooperative fashion to achieve structural relaxation. To further confirm the free-volume effect that might be responsible for the measured slow dynamics of strongly confined colloids, we examine the wall effect on in-plane volume fraction of confined PMMA suspensions as shown in Figs. 2(c) and 2(d). We observe that the two-dimensional (2D) volume fraction of midplanes that are 2–3 particle layers away from the substrates remains relatively constant for thick films, i.e., $H/d \approx 17$. This suggests that the increase in friction due to the sintered PMMA results in a greater particle density at the walls, at a cost of disturbing the layering, thus the effect of the depletion layer is reduced. At $H/d \approx 5$, we observe a considerable increase in volume fraction at the midplanes. The sharp increase in volume fraction for certain values of film thickness where structural arrest is observed suggest an important observation, while local packing fraction at the midplane of the confined film may show a sharp increase, the overall volume fraction of the film is essentially constant. Therefore, our findings suggest dramatic spatial variations in densities for the confinement induced glass transition. These variations inherently govern the slowing down of dynamics and subsequent arrest, similar to supercooled liquids close to T_g.

The MSD data naturally raise the question: How does confinement alter structural relaxation? To gain quantitative insight into film thickness dependence of structural relaxation, we compute the "self-part," $F_s(q,\tau)$ of the intermediate scattering function (ISF) in 2D, which is defined as

$$\langle F_s,(q,\tau)\rangle = \mathrm{Re}\left\{\frac{1}{N}\sum_{j=1}^{N}\langle \exp(iq[r_j(t)-r_j(\tau)])\rangle\right\} \qquad (2)$$

where the 2D ISF is computed at $q=2\pi/d$ ($d=1.2$ μm) and $[r_j(t)-r_j(\tau)]$ is the in-plane displacement of the jth particle averaged over all initial times, t_0 [24,25]. The 2D ISF is the spatial Fourier transform of the self-part of the van Hove correlation function, $G_s(r,\tau)$, which indicates the fraction of particles located in a radially distributed region from r to $r+dr$ at a given τ, provided that the particles are initially located at their respective origins at t_0. The normalized self-ISF, defined as $f(q,t)=\langle F_s(q,\tau\rangle/\langle F_s(q,0)\rangle$, where $\langle F_s(q,0)\rangle$ is the static structure factor, is shown in Fig. 3 for confined PMMA suspensions of $\phi=0.43$ and 0.57. The decay of $f(q,\tau)$ is fast for $H/d>25$ and the simple exponential decay indicates that all particles relax independently. In contrast, two-step decay, characteristic of supercooled liquids, is observed at $H/d\leqslant 17$. It is intriguing to see that the normalized ISF does not decay to zero over ~ 0.5 h, suggesting a transition from a fluid to a "supercooled" regime, where the intermittent process of cage trapping and subsequent cage rearrangement retards the decay of the ISF. When film thickness is further reduced to $H/d \approx 4-5$, no long-time decay in $f(q,\tau)$ is observed, which is similar to the behavior of bulk colloidal glasses [12]; the ISF approaches time invariance, reflecting the nonergodic state of confined colloidal suspensions where particles remain permanently trapped in cages formed by their neighbors.

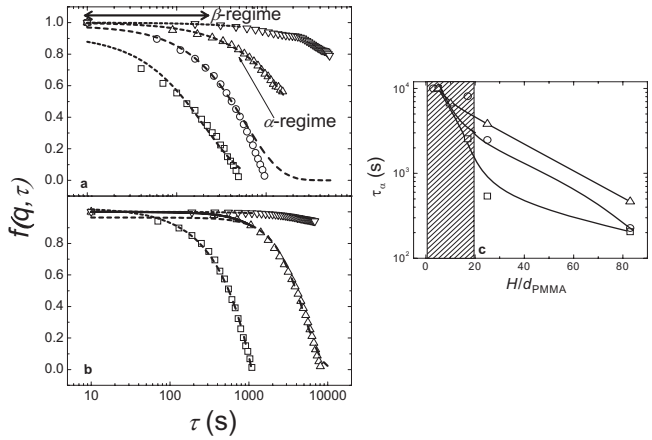

FIG. 3. Normalized self-intermediate scattering function (ISF), $f(q,\tau)$, of PMMA suspension for (a) $\phi=0.43$. The decay is increasingly stretched as film thickness decreases from the bulk ($H/d \approx 100$) (squares), and $H/d=25$ (circles) and 17 (upper triangles), until nonergodicity sets in at $H/d=4$. Similar scaling behavior is observed for (b) $\phi=0.57$, for the bulk ($H/d \approx 100$) (squares), and $H/d=17$ (upper triangles) and 5 (down triangles). (c) Logarithmic α relaxation time, τ_α, is plotted against normalized film thickness, H/d, for $\phi=0.43$ (squares), 0.49 (circles), and 0.57 (triangles). The shaded area indicates the divergence of τ_α.

It is of great interest to examine the time scales of structural relaxation in confined colloidal suspensions, which can be extracted from the normalized ISF, $f(q,\tau)$. The β-relaxation time can be clearly identified by the end of the plateau in $f(q,\tau)$, while the α-relaxation time can be determined by fitting the Kolrausch-Williams-Watts (KWW) formula [9], $f(q,\tau)=\exp[-(\tau/\tau_\alpha)^\beta]$, to the normalized ISF. We define the onset of the α-relaxation process as the time scale when $f(q,\tau)$ becomes equal to e^{-1}. As shown in Fig. 3(c), the α-relaxation time, obtained from KWW fitting for varied bulk volume fractions, clearly exhibits a strong dependence on film thickness. The α-relaxation time diverges as film thickness approaches $H/d<17$, indicating the onset of the glass transition where the α-relaxation process is suspended [12].

The self-ISF is a dynamic quantity that indicates the preserved fluctuations of particles around their initial positions for all times. However, it is of great importance to deduce how system memory [26] and hopping events [27] may affect structural relaxation of a thin film. Bearing this in mind, we analyze the autocorrelation function associated with the ISF, which is computed as

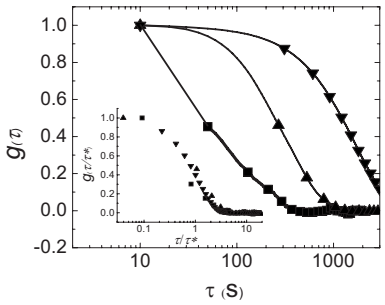

FIG. 4. Autocorrelation function, $g(\tau)$, of confined colloidal suspension of $\phi=0.57$ for the bulk (squares), $H/d=17$ (upper triangles) and $H/d=5$ (down triangles). Inset: Collapsed autocorrelation function to confirm the scaling behavior. The data were collapsed into a single curve based on their respective time constants, $\tau_c=109$, 294, and 1524 s, for the bulk, $H/d=17$ and $H/d=5$, respectively.

$$g(\tau) = \frac{\langle F_s(q,t_0)F_s(q,\tau)\rangle}{\langle F_s(q,t_0)F_s(q,t_0)\rangle} \tag{3}$$

and averaged over all initial times, t_0. Our autocorrelation function reveals the time scale at which cage rearrangement occurs, as this information is not accessible with the self-intermediate scattering function that is usually a common probe for slow dynamic processes. As shown in Fig. 4 for confined PMMA suspension of $\phi=0.57$, the correlation time is consistently shifted to longer lag times as film thickness is reduced. In addition, the cage rearrangement time scales can be obtained from the time constants associated with the exponential decay of $g(\tau)$. For $H/d>25$ we find that the cage rearrangement time, $\tau_c=109$ s, roughly corresponds to the upturn in the MSD. Similar behavior is observed at $H/d \approx 17$ and ≈ 5, where cage rearrangement becomes retarded as τ_c shifts to 294 s and 1524 s, respectively.

In summary, we have shown dramatic change in particle mobility and structural relaxation of colloidal suspensions under confinement. In particular, it is clear that glassy dynamics can be induced by decreasing film thickness while volume fraction remains constant. This phenomenon is primarily due to a reduction in film thickness of colloidal suspensions, which restricts considerable changes in the topology of caged colloidal particles upon confinement and is responsible for the divergence of the α-relaxation times obtained from the normalized intermediate scattering function.

We thank E. R. Weeks, H.-C Chang, and E. J. Maginn for fruitful discussions. This work was supported by the US Department of Energy, Division of Materials Science (Grant No. DE-FG02-07ER46390) and the National Science Foundation (Grant No. CBET-0730813). Partial equipment support was provided through the Equipment Renewal and Restoration Program at the University of Notre Dame.

[1] A. J. Liu and S. R. Nagel, in *Jamming and Rheology*, edited by A. J. Liu and S. R. Nagel (Taylor & Francis, New York, 2001).
[2] R. Stinchcombe, in *Jamming and Rheology* (Ref. [1]).
[3] M. M. Teeter, A. Yamano, B. Stec, and U. Mohanty, Proc. Natl. Acad. Sci. U.S.A. **98**, 11242 (2001).
[4] Z. Sun, J. Zhou, and R. Ahuja, Phys. Rev. Lett. **98**, 055505 (2007).
[5] G. Adam and J. H. Gibbs, J. Chem. Phys. **43**, 139 (1965).
[6] C.-Y. Wang and M. D. Ediger, J. Phys. Chem. B **103**, 4177 (1999).
[7] W. K. Kegel and A. van Blaaderen, Science **287**, 290 (2000).
[8] E. R. Weeks, J. C. Crocker, A. C. Levitt, A. Schofield, and D. A. Weitz, Science **287**, 627 (2000).
[9] W. Götze and L. Sjogren, Transp. Theory Stat. Phys. **24**, 801 (1995); W. Götze, J. Phys.: Condens. Matter **11**, A1 (1999).
[10] D. R. Reichman and P. Charbonneau, J. Stat. Mech.: Theory Exp. 05013, 1 (2005).
[11] P. N. Pusey and W. van Megen, Nature (London) **320**, 340 (1986).
[12] W. van Megen and S. M. Underwood, Phys. Rev. Lett. **70**, 2766 (1993); Phys. Rev. E **49**, 4206 (1994).
[13] C. J. Ellison and J. M. Torkelson, Nat. Mater. **2**, 695 (2003).
[14] Z. Fakhraai and J. A. Forrest, Phys. Rev. Lett. **95**, 025701 (2005).
[15] J.-Y. Park and G. B. McKenna, Phys. Rev. B **61**, 6667 (2000).
[16] F. Varnik, J. Baschnagel, and K. Binder, Phys. Rev. E **65**, 021507 (2002).
[17] A. L. Demirel and S. Granick, Phys. Rev. Lett. **77**, 2261 (1996).
[18] Y. Zhu and S. Granick, Langmuir **19**, 8148 (2003).
[19] A. D. Dinsmore, E. R. Weeks, V. Prasad, A. C. Levitt, and D. A. Weitz, Appl. Opt. **40**, 4152 (2001).
[20] J. C. Crocker and D. G. Grier, J. Colloid Interface Sci. **179**, 298 (1996).
[21] See EPAPS Document No. E-PLEEE8-76-R11712 for supplemental experimental procedure and additional images showing the glasslike structure of confined PMMA thin films at varied volume fractions. For more information on EPAPS, see http://www.aip.org/pubservs/epaps.html
[22] E. R. Weeks and D. A. Weitz, Phys. Rev. Lett. **89**, 095704 (2002).
[23] Our analysis shows that $\langle x^2\rangle \approx \langle y^2\rangle$, which is not shown here. Because of slower scanning along the z direction, we focus on the in-plane particle dynamics parallel to the confining walls (the xy plane) in this work.
[24] R. Yamamoto and A. Onuki, Phys. Rev. E **58**, 3515 (1998).
[25] O. Dauchot, G. Marty, and G. Biroli, Phys. Rev. Lett. **95**, 265701 (2005).
[26] T. Srokowski and A. Kamínska, Phys. Rev. E **74**, 021103 (2006), and references therein.
[27] P. Ribiere P. Richard, R. Delannay, D. Bideau, M. Toiya, and W. Losert, Phys. Rev. Lett. **95**, 268001 (2005).